EXPERIMENTAL AND NUMERICAL STUDIES OF STRUCTURAL PERFORMANCE OF NOTCH DAMAGED STEEL BEAMS

SAID ELKHOLY[1] and BILAL EL-ARISS[1]

[1]Civil and Environmental Engineering Department, United Arab University, Al Ain, UAE

Performance of notch damaged unrepaired steel I-shaped beam specimens was examined experimentally and numerically simulated using finite element modeling. Nine U-shaped notch damaged specimens and one control beam specimen were considered. The nine unrepaired laterally unsupported I-shaped full-scale steel specimens were tested in two-point loadings and the parameters considered in the study were the size and location of the notch. The notch size was 30 mm, 40 mm, and 60 mm in depth with constant opening width of 20 mm. The location of the notch was at one-quarter, one third, and middle of the specimen clear span. All pre-damaged specimens had notches on one side of the tension flange with respect to the beam web except for two specimens where two notches were cut at the middle of the specimen clear span on both sides of the tension flange. The test specimens were modeled analytically using three-dimensional models of the bare-steel I-shaped specimens for comparison of the analytical predictions with experimental results. The test results showed the strength of the notched beams was hardly affected by the notch size or location. However, the stiffness of the beams was slightly decreased as the notch got closer to the mid-span with increased ductility. The corresponding analytical results were in good agreement with the test data.

Keywords: Laboratory testing, FE simulation, I-shaped members, Stiffness, Load bearing capacity.

1   INTRODUCTION

Kim and Brunell (2011) and Kim and Harries (2012) explored the CFRP restoration approaches for notch damaged steel beams. The impact of the notch shapes was considered numerically to find the relations between CFRP restoration approaches and initial damage in the steel beams tested in flexure. Siwowski and Siwowska (2018) investigated the structural behavior of CFRP plate-strengthened steel beams. Four different shapes of strengthening steel plates with notch under fatigue load. They showed the possibility of extending the fatigue life of steel plate approximately four times with non-prestressed plates and, in some cases, fully stopping the crack growth by means of prestressed plates. Elchalakani (2016) offered investigational results of corroded steel circular hollow sections (CHS) repaired with CFRP sheets and tested under large displacements. The author showed that corrosion level can affected the percentage in combined flexural and bearing strength of the CHS. Kadhim (2012) studied the behavior of CFRP plate-repaired continuous steel beam. The analytical results specified that for CFRP repairing plate lengths in hogging and sagging regions of the beam of around 60% and 40% of beam span length, respectively, the ultimate strength increase rate diminished. Yu *et al.* (2011) established a bond

slip model to predict the debonding of FRP laminates used to strengthen steel beams considering the effects of adhesive thickness on the bond strength, laminate thickness, and bond length and strength. It was determined that the bond strength between the strengthening FRP laminates and steel beams can be increase as a result of decreasing the laminate thickness and modulus, minimizing the adhesive thickness, or increasing the bond length. Chen *et al.* (2018) experimentally observed the fatigue performance of damaged steel rectangular hollow section (RHS) beams. The test data indicated that the used CFRP sheets with high modulus increased the RHS beam fatigue life. Tavakkolizadeh and Saadatmanesh (2003a and 2003b) and Photio *et al.* (2004) studied the behavior of damaged steel-concrete composite steel girders repaired with CFRP sheets under static loading. Test results revealed that epoxy bonded CFRP sheets could restore the stiffness and ultimate load-carrying capacity and of repaired girders. Comparison between experimental and numerical modeling showed that the traditional methods of analysis of composite beams were conservative. Deng *et al.* (2018) applied mixed-mode cohesive approach to imitate CFRP- strengthened notch damaged steel beams. Study revealed that although the beam strength was increased, the ductility reduced as the notch extent increase and debonding mode of failure premature occurred. It is clear that previous works show that researchers have mostly proposed retrofitting techniques to damaged steel members and investigated the rehabilitated member performance. The objective of this study is to examining the flexural behavior of unrepaired laterally unsupported notch damaged steel beams.

2   EXPERIMENTAL PROGRAM

A program for testing a total of ten W-shaped steel beams was prepared. One undamaged (control) and nine artificially U-shaped notch damaged beams were instrumented and tested in flexural. The notch was cut in the beam bottom flange and all beams were left unrepaired and laterally unsupported while tested. The notch size was 30 mm, 40 mm, and 60 mm in depth with constant width of 20 mm and was cut on one side of the beam bottom (tension) flange with respect to the beam web. All of the beams had clear span of 1800 mm between the support and a total length of 2000 mm, Figure 1. The location of the notch was at one-quarter, one-third, and middle of the specimen clear span, as shown in Figure 2 for notch at middle of the beam.
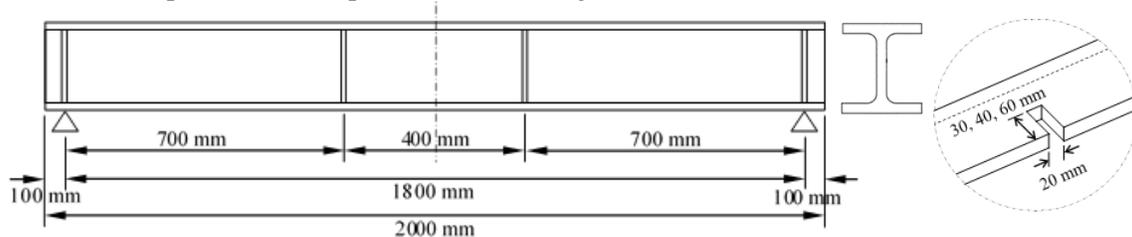

Figure 1. Details of a typical notch damaged I-beam specimen.
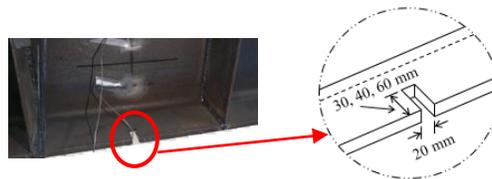

Figure 2. Location of notch in the beam bottom flange.

The w-shape steel beams were of W 203 x 203 x 52 sections with a web height and thickness of 206 mm and 7.9 mm, respectively, and a flange width and thickness of 204 mm and 12.6 mm,

respectively, and 46.1 kg/m mass. The beam specimens were web-stiffened to avoid web crippling at the support locations and at the two loading point locations which are 400 mm apart and 700 mm away from supports, as presented in Figures 1 and 3.

Figure 3. The beams with vertical stiffeners over supports and under loading points.

2.1 Material Properties and Test Matrix

The mechanical properties of the studied steel W-shaped specimens were obtained from standard tensile coupon test. The average ultimate and yielding strength values obtained were 441 MPa and 294 MPa, respectively. The damaged beams were divided into three groups and are shown in Table 1.

Table 1. Test Matrix.

Group (Location of Notch)*	Length of Notch (mm)	Specimen Name
C	0	C-NG-0
Q	30	QS-30
	40	QS-40
	60	QS-60
T	30	TS-30
	40	TS-40
	60	TS-60
M	30	MS-30
	40	MS-40
	60	MS-60

C=control beam (undamaged); Q=notch at beam quarter span; T=notch at beam one-third span; M=notch at beam mid-span.
NG-0=no notches (0 depth); S=single notch on one side of bottom flange.
Specimen Name - example: *QS-30=single notch of 30 mm depth on one side of bottom flange at beam quarter span.*

2.2 Instrumentation of Test Setup

The steel W-shaped beams were tested in four-point bending set-up with two point loads applied. The beams had of clear span between the supports of 1800 mm. The two applied point loads were 200 mm on each side of the centerline of the beam and 700 mm from the supports, Fig. 1. The control beam and notch damaged beams were left unrepaired; however, to avoid web crippling of the beams during testing, the beams were web-stiffened with vertical stiffeners under the load application points and above the supports. All steel beam specimens were loaded in a displacement-control mode at a rate of 2 mm/min and were kept laterally unsupported during testing, Fig. 2 and 3. The beam were equipped and instrumented with strain gauges, for strain readings, and Linear Variable Differential Transformers (LVDT), for deflection measurements. The strain gauges were bonded to the outer surface of top and bottom flanges and the web of the beams at locations. The LVDTs were located below the bottom flange at the load application points and at centerline of the beam, as shown in Figure 4.

Figure 4. Installation of strain gauges and placement of LVDT's.

2.3 Finite Element Simulation

Finite element simulation of the tested beams was carried out. Three dimensional models of were generated to simulate the tested W-shaped steel beams numerically up to starting of lateral torsional buckling as the beams were not laterally supported. The models were produced using finite element (FE) analysis program, ATENA. Three types of three-dimensional solid elements are provided by ATENA-3D: tetrahedral elements (CCIsoTetra), brick elements (CCIsoBrick), and wedge elements (CCIsoWedge). After several trials of tuning the FE mesh, the Tetrahedral 3-D (T3D) solid element was found to be the most appropriate element that best explained the behavior of the specimens and; therefore, was used to generate the FE models. A displacement-controlled incremental loading method was employed in the FE analysis. The standard Newton-Raphson iterative solution method implemented in ATENA was adopted in the analysis. A schematic sketch of the beams modeling is shown in Figure 5.
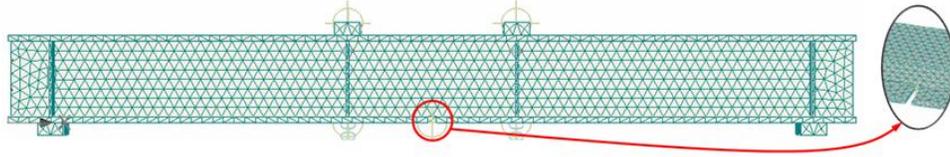

Figure 5. Finite element modeling of the testes W-shaped beams.

3 DISCUSSION OF EXPERIMENTAL AND NUMERICAL RESULTS

Figure 6 presents the experimental load-deflection relations of the three groups of the beams, Q, T, and M separately. The figure shows that group Q specimens had the same stiffness regardless of the notch size. Group T specimens demonstrated a slight decrease in the specimen stiffness as the notch size increased due to notch location. Group M revealed more noticeable decrease in the beam stiffness as the notch location had more impact. However, the ductility of the three group specimens had the same pattern where the largest ductility was for the highest notch size, 60 mm.
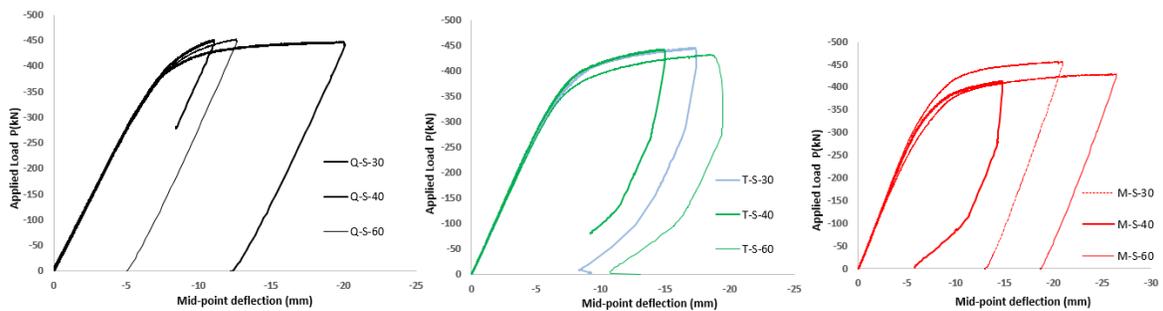

Figure 6. Load-deflection curves.

Figure 7(a) depicts the experimental load-deflection relations for the tested beams. It can be seen that when the notch was at quarter of the span, the beam had the highest load carrying capacity and the least ductility. When the notch was at third span of the span, the beam load carrying capacity decreased while the ductility increased. The beam had the highest ductility when the notch was at the mid-span but the load carrying capacity was the least. This can be attributed to the beam failure mode as a result of the notch location. More specifically, when the notch is at furthest location from the beam centerline (quarter of span), the beam the beam prematurely twisted at low deflection value. On the other hand, when the notch was at the mid-span, the beam was able to sustain more deflection due to beam symmetry effect until lateral torsional buckling occurred. The beam behavior was somewhat in between the latter cases when the notch was at third of the beam span. Figure 7(b) shows the load-top and bottom strain relationships of group T specimens.
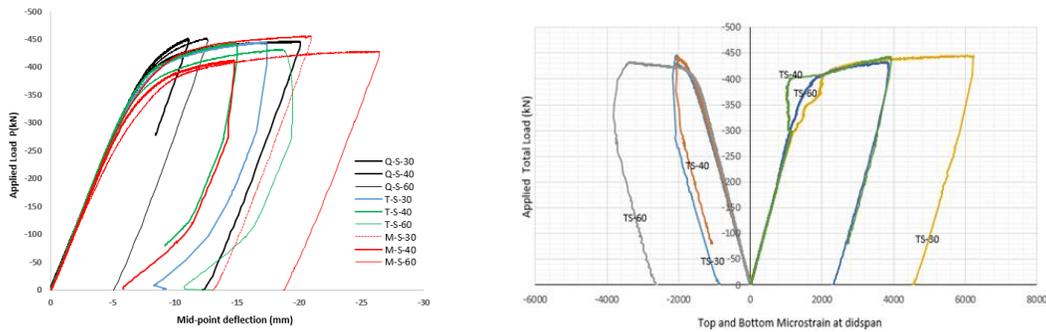

Figure 7. (a) Load-deflections of all beams, (b) load-strain curve for TS-30, 40, and 60 specimens.

Figures 8 shows the finite element deflection of specimen MS-40. It is clear that the beam numerically predicted behavior matched the beam experimental behavior in terms of buckling failure and location. Both numerical and experimental buckling occurred in the back top flange of the beams simultaneously with plastic deformation arose in the front notch in the bottom flange.
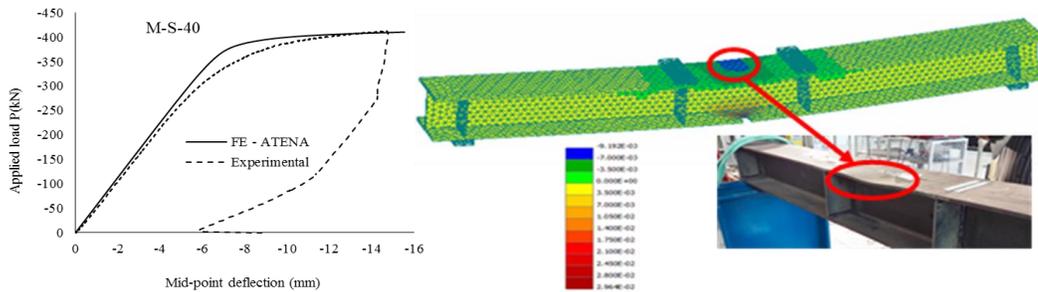

Figure 8. Comparison of FE analysis and experimental results and buckling in specimen M-S-40.

Figure 9 shows the numerical plastic strain in the notch at different loading steps of the test and failure buckling in specimen MS-40. It is obvious from the figure the numerical bucking failure predicted was in agreement with observed experimental. This confirmed the predicted numerical bucking failure. The test results; therefore, verified the accuracy of the numerical simulation of the tested beams generated in this study. Also, both experimental and numerical outputs showed the same pattern of plastic strain occurring in the notch in the front bottom flange buckling arising in the back of the top flange of the beam.
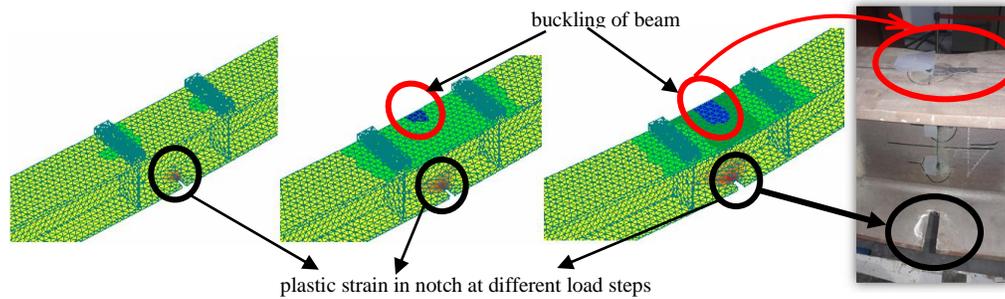
Figure 9. Plastic strain in notch at different loading step and buckling in specimen MS-40.

4 CONCLUSION

Experimental and numerical investigation were performed on ten I-shape steel beams with nine beams were artificially u-shaped notch damaged. The notch location had more effects on the beam behavior, ductility, and failure mode than the notch size effects. The finite element simulations and predictions were in agreement with the experimentally observed results.

References

Chen, T., Wang, X., and Qi, M., Fatigue improvements of cracked rectangular hollow section steel beams strengthened with CFRP plates, *Thin-Walled Structures*, 122, 371-377, 2018.

Deng, J., Li, J., Wang, Y., and Xie, W., Numerical study on notched steel beams strengthened by CFRP plates, *Construction and Building Materials*, 163, 622-633, 2018.

Elchalakani, M. (2016). Rehabilitation of corroded steel CHS under combined bending and bearing using CFRP, *Journal of Constructional Steel Research*, 125, 26-42.

Kadhim, M. M. A., Effect of CFRP plate length strengthening continuous steel beam, *Construction and Building Materials*, 28(1), 648-652, 2012.

Kim, Y. J. and Brunell, G., Interaction between CFRP-repair and initial damage of wide-flange steel beams subjected to three-point bending, *Composite Structures*, 93(8), 1986-1996, 2011.

Kim, Y. J. and Harries, K. A, Predictive response of notched steel beams repaired with CFRP strips including bond-slip behavior, *International Journal of Structural Stability and Dynamics*, 12(01), 1-21, 2012.

Photiou, N., Hollaway, L. C., and Chryssanthopoulos, M. K., Strengthening of an artificially degraded steel beam utilising a carbon/glass composite system, *In Advanced Polymer Composites for Structural Applications in Construction* (pp. 274-283), 2004.

Singh, A., Smith, H., and Shoura, M. M., Evaluation of Change: A Case Study, *International Journal of Project Management*, Elsevier, 24(4), 337-348, May, 2006.

Siwowski, T. W. and Siwowska, P., Experimental study on CFRP-strengthened steel beams, *Composites Part B: Engineering*, 149, 12-21, 2018.

Tavakkolizadeh, M., and Saadatmanesh, H., Repair of damaged steel-concrete composite girders using carbon fiber-reinforced polymer sheets, *Journal of Composites for Construction*, 7(4), 311-322, 2003a.

Tavakkolizadeh, M., and Saadatmanesh, H., Strengthening of steel-concrete composite girders using carbon fiber reinforced polymers sheets, *Journal of Structural Engineering*, 129(1), 30-40, 2003b.

Yu, Y., Chiew, S. P., and Lee, C. K., Bond failure of steel beams strengthened with FRP laminates–Part 2: Verification, *Composites Part B: Engineering*, 42(5), 1122-1134, 2011.